COMMUNICATIONS CHEMISTRY

ARTICLE

https://doi.org/10.1038/s42004-018-0099-7 OPEN

Triple photochemical domino reaction of a tetrafluorostilbene terminating in double fluorine atom transfer

Takashi Murase [1], Chikako Matsuda[1], Kiyohiro Adachi [2,3], Tomohisa Sawada [3] & Makoto Fujita [3]

In domino reactions, the product formed in one step undergoes a subsequent transformation under identical reaction conditions. Owing to the spontaneous nature of these reactions, it is difficult to isolate the key intermediates, and these are thus usually presumed. Here we perform a photoinduced domino reaction consisting of three photochemical steps. First, oxidative photocyclisation of a tetrafluorostilbene derivative generates tetrafluoro[7]helicene, which readily undergoes a photoinduced intramolecular Diels–Alder reaction. The resulting product then undergoes a double fluorine atom transfer under the same photochemical conditions. As a result, the four originally adjacent fluorine atoms are separated into two pairs in the final product. One advantage of a photochemical domino process over a thermal one is that the process can be suspended and restarted. Hence, precise control of the irradiation time allows us to isolate the thermally stable intermediates and characterise them using X-ray crystallography, thus confirming the until-now putative domino process.

[1] Faculty of Science, Yamagata University, Kojirakawa-machi, Yamagata, Yamagata 990-8560, Japan. [2] Instrument Center, Institute for Molecular Science, National Institutes of Natural Sciences, 5-1, Higashiyama, Myodaiji-cho, Okazaki, Aichi 444-8787, Japan. [3] Department of Applied Chemistry, School of Engineering, The University of Tokyo, Hongo, Bunkyo-ku, Tokyo 113-8656, Japan. Correspondence and requests for materials should be addressed to T.M. (email: tmurase@sci.kj.yamagata-u.ac.jp)

Domino reactions are defined as two or more consecutive transformations under identical reaction conditions, in which the subsequent reactions take place at the functionalities formed in the previous steps without the addition of further reagents or catalysts[1–3]. This type of reaction is represented in the biosynthesis of lanosterol from (*S*)-2,3-oxidosqualene[4], in which sequential intramolecular cyclisations occur as a result of the organised and proximal reaction sites of the intermediate in each step. Given that domino reactions proceed without the isolation of any intermediates, judicious planning is required to predict the reaction pathways by combination of known transformations. Nevertheless, domino reactions sometimes bring about unprecedented transformations. For example, a 1,3-diyne with a tethered alkynyl diynophile undergoes an intramolecular hexadehydro-Diels–Alder reaction[5] to form a highly reactive benzyne intermediate, which is quickly trapped by a cycloalkane solvent[6,7]. This trap reaction is an intermolecular double hydrogen atom transfer from the cycloalkane 2H-donor to the benzyne 2H-acceptor, and produces the corresponding cycloalkene and substituted benzene. If the benzyne intermediate is trapped intramolecularly by another tethered 1,3-diyne, a naphthyne is formed as a second aryne intermediate[8]. The intramolecular aryne formations are repeated until the intermediate is trapped by an external arynophile.

To clarify the mechanism of a domino process that involves an unprecedented transformation, direct isolation of the key intermediates is required. However, this is challenging because the intermediates are usually unstable and highly reactive. We envisage that if each step in the domino process proceeds under identical external stimuli, thermally stable intermediates could be isolated by removing the applied stimuli. Consequently, we would be able to directly visualise and discuss the whole process without having to make any assumptions, as if taking a snapshot of the intermediate at a given reaction time[9].

Here, we perform a photoinduced domino reaction consisting of three photochemical steps (Fig. 1). First, the oxidative photocyclisation of stilbene derivative **1** bearing a tetrafluorobenzene ring at the terminal affords 1,2,3,4-tetrafluoro[7]helicene (F_4-[7]helicene; **2**), which readily undergoes a formal intramolecular Diels–Alder reaction induced by photoirradiation. Then, resulting product **3** undergoes a double fluorine atom transfer to afford **4** under the same photochemical conditions. As a result, the four neighbouring fluorine atoms on the same benzene ring of **1** are separated into two fluorine pairs in a single photochemical operation. In this triple photochemical domino process, intermediates **2** and **3** are thermally stable and can thus be characterised by X-ray crystallography, which allows the elucidation of the otherwise putative domino process.

Results

Photoirradiation of tetrafluorostilbene 1. Photochemical electrocyclisation of stilbene derivatives followed by thermal in situ dehydrogenation with iodine is the standard protocol for synthesising a variety of helicene homologues[10–14]. Previously, we have demonstrated that an elongated stilbene derivative with six vinylene spacers undergoes oxidative photocyclisation at six separate positions to afford [16]helicene, the longest known carbohelicene[15]. We applied the same protocol to a toluene solution of F_4-stilbene **1** (0.20 mM) using a high-pressure Hg lamp (Fig. 2a). After 30 min irradiation at 30 °C, the starting material was completely consumed. However, intended F_4-[7]helicene **2** was not obtained, and instead, bridged compound **4** was isolated in 20% yield. Even when the reaction was conducted at 0 °C for 30 min, **2** was not obtained (**4**; 14% yield). The product yield of **4** was increased to 40% by irradiation for 10 min at 50 °C.

The structure of **4** was unambiguously determined by X-ray crystallographic analysis (Fig. 2b and Supplementary Figure 3). The bottom bicyclooctane framework is fused with the lateral benzene ring and the vertical [4]helicene moiety, generating a spiro-carbon at the centre. Intriguingly, two fluorine atoms, which were originally located on the terminal benzene ring of **1**, were transferred to the bicyclooctane ring with syn-stereochemistry. On the basis of the crystal structure, we next investigated the solution structure of **4** by NMR spectroscopy (Fig. 2c). The NMR signal of the endo proton H_i ($\delta = 5.14$ ppm) is a doublet of triplets with a large geminal F_2–H_i coupling ($^2J_{FH} = 51.0$ Hz) and small vicinal H_j–H_i and F_1–H_i couplings (*gauche* $^3J_{HH} = {}^3J_{FH} = 3.4$ Hz), whereas the signal of the bridgehead proton H_j ($\delta = 5.34$ ppm) is a doublet of triplets with small H_i–H_j and F_2–H_j couplings. The *cis*-vicinal F_1–F_2 coupling (*cis* $^3J_{FF} = 20.2$ Hz) was recorded by ^{19}F NMR spectroscopy.

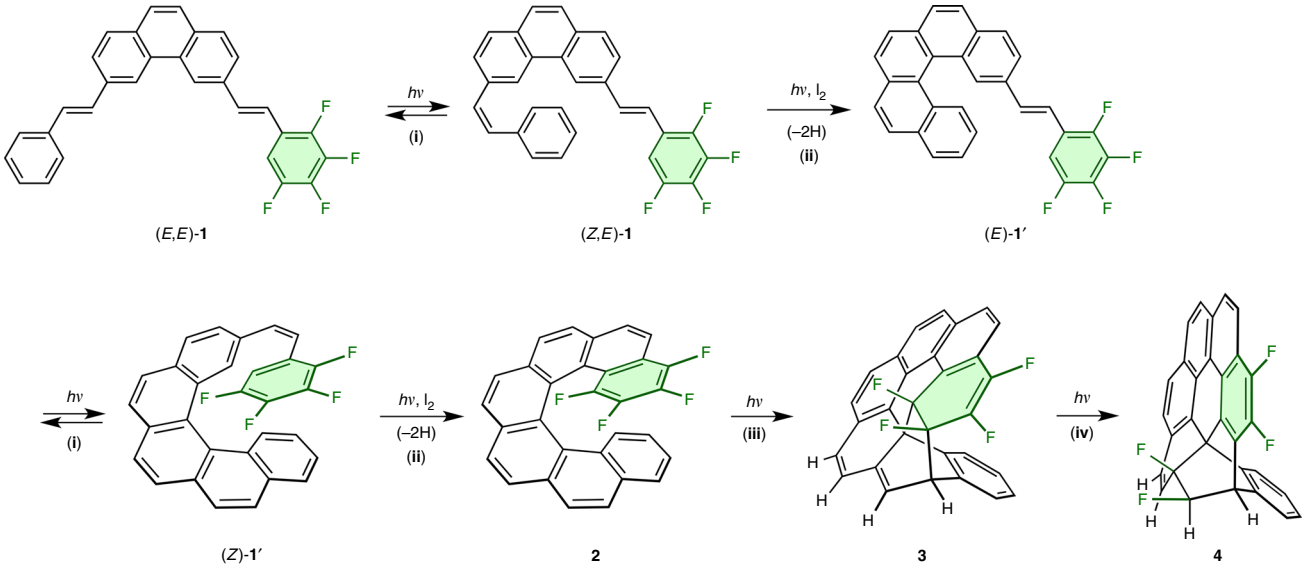

Fig. 1 Triple photochemical domino reaction. **i** *E*/*Z*-Photoisomerisation. **ii** [6π]-Electrocyclisation followed by dehydrogenation (oxidative photocyclisation). **iii** [4π + 2π]-Cycloaddition (photoinduced Diels–Alder reaction). **iv** [2σ + 2σ + 2π]-Double group transfer reaction (photoinduced dyotropic rearrangement). The number of participating orbital electrons is shown in square brackets. In the oxidative photocyclisation from **1** to **1′**, the (*E*,*Z*) and (*Z*,*Z*) isomers of **1** are also present but not shown for simplicity

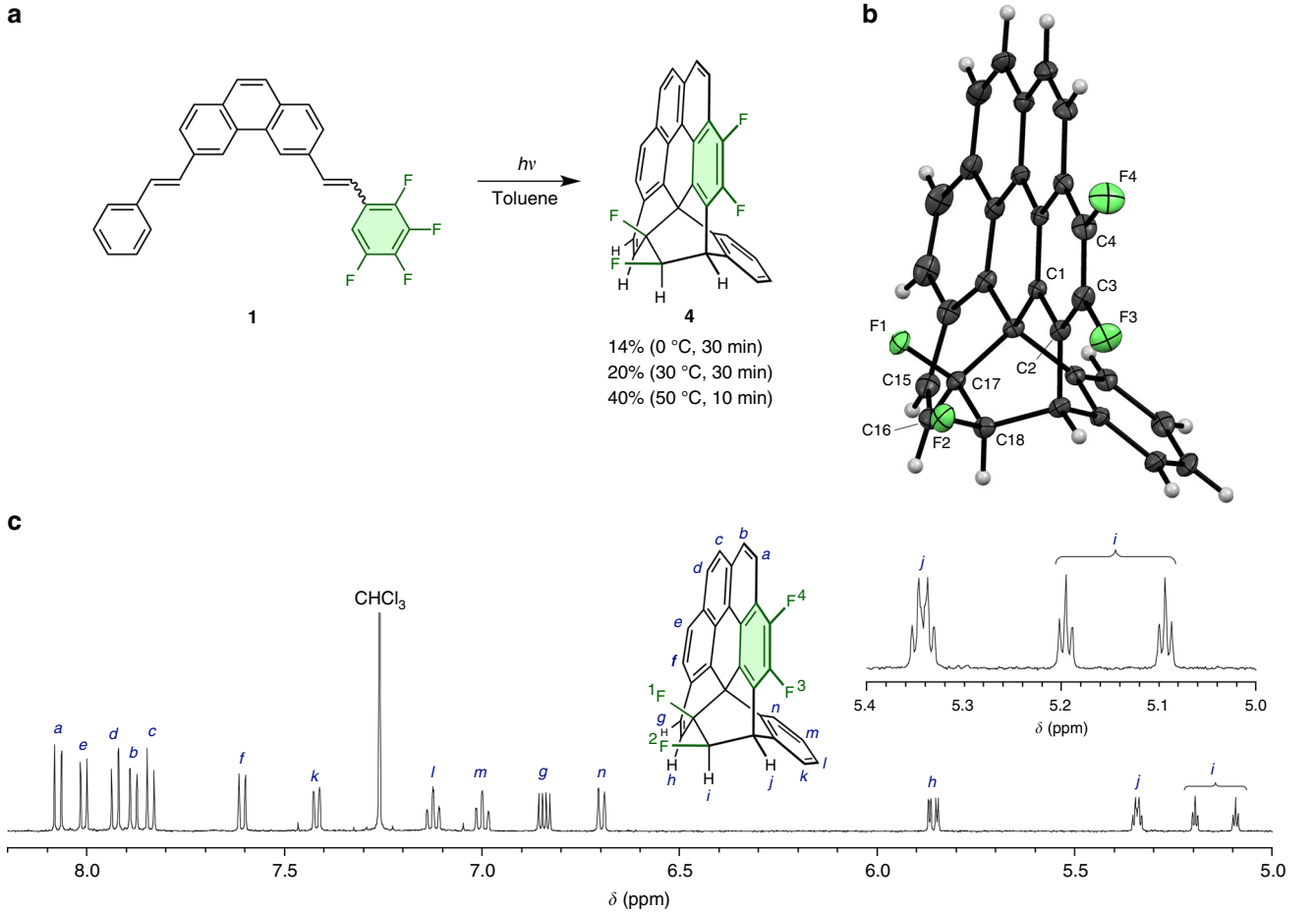

Fig. 2 Synthesis and characterisation of **4**. **a** Transformation of **1** to **4** under UV light irradiation in the presence of I_2 (oxidant, 2.2 equiv.). **b** ORTEP drawing of the X-ray crystal structure of **4** (thermal ellipsoids at the 50% probability level). Only one enantiomer is shown here but the crystal structure contains both enantiomers. Selected interatomic distances (Å) and torsion angles (°): C17–F1, 1.407(2); C18–F2, 1.398(2); C3–F3, 1.356(2); C4–F4, 1.348(2); C1–C2, 1.378(2); C15–C16, 1.336(3); C16–C17, 1.507(3); C17–C18, 1.555(2); F1–C17–C18–F2, 2.3(2); C15–C16–C17–F1, 83.7(2). **c** ^{1}H NMR spectrum (500 MHz, 298 K, $CDCl_3$) of **4**. The characteristic signal region (5.0–5.4 ppm) is highlighted in the inset. Note that the endo proton H_i appears as a doublet of triplets with a large geminal coupling constant of 51.0 Hz at 5.14 ppm

Clearly, multi-step transformations occurred to generate **4** from **1** under photoirradiation. To closely follow the progress of the photochemical process, we strictly controlled the irradiation time (Supplementary Figure 4). A shorter irradiation time (2 min, 50 °C) allowed us to isolate F_4-[7]helicene **2** in 7% yield, together with unreacted **1** (75% yield). Another intermediate, **3**, was obtained by irradiation for 5 min at 50 °C (isolated yields of **1**: 13%; **2**: 18%; **3**: 14%; **4**: 8%). Intermediates **2** and **3** were thermally stable even in refluxing toluene (~120 °C). These results clearly demonstrate that, in addition to the first (**1** → **2**) step, the second (**2** → **3**) and third (**3** → **4**) steps proceed photochemically and successively under the same conditions (Fig. 1). The triple photochemical domino reaction starts with the photochemical [6π]-electrocyclisation of **1** through facile *E*/*Z*-photoisomerisation at two separate positions to give an unstable dihydrophenanthrene intermediate. In the absence of iodine, the domino process does not start because the dihydrophenanthrene intermediate returns to **1** without being oxidised. The phenanthrene formation at the F_4-styryl terminal was slower than that at the unsubstituted styryl terminal: [5]helicene bearing the F_4-styryl group **1′** was isolated (~15%) from the reaction mixture after 5 min irradiation (Supplementary Figure 5).

The structures of domino intermediates **2** and **3** were also confirmed by X-ray crystallographic analysis. Despite our extensive efforts to optimise the crystallisation conditions for **2**, crystal twinning inevitably occurred. Intermediate **2** formed racemic crystals in the triclinic space group $P\bar{1}$ with four independent molecules (i.e., two *P* and two *M* enantiomers) in the asymmetric unit (Fig. 3a and Supplementary Figure 1). In the crystal, the *P* and *M* enantiomers are alternatively arranged without intermolecular aromatic–aromatic interactions. The C–C bonds in the inner helix have single bond character (e.g., C25–C26, 1.455–1.467 Å), whereas those in the outer helix have double bond character (e.g., C18–C19, 1.344–1.355 Å); these are typical characteristics of helicene-like molecules. The shortest C···C contact is found between C1 and C26 (2.901–2.935 Å) in the inner helix, and these atoms are connected by the subsequent transformation. The centroid distance between the two terminal benzene rings in crystalline F_4-[7]helicene **2** (3.57–3.70 Å) is shorter than that in crystalline unsubstituted [7]helicene (3.78–3.89 Å)[16–20], which indicates favourable stacking interactions between the upper F_4-benzene and the lower unsubstituted benzene moieties at the terminals[21–24].

Intermediate **3** exhibited spontaneous resolution of enantiomers and crystallised in the non-centrosymmetric space group, monoclinic $P2_1$ (Fig. 3b and Supplementary Figure 2). The X-ray structure of **3** clearly illustrates that an intramolecular [4π + 2π]-cycloaddition of **2** takes place between the second distal benzene ring as a diene and the terminal electron-deficient F_4-benzene ring as a dienophile to generate the C1–C26 and C2–C19 bonds.

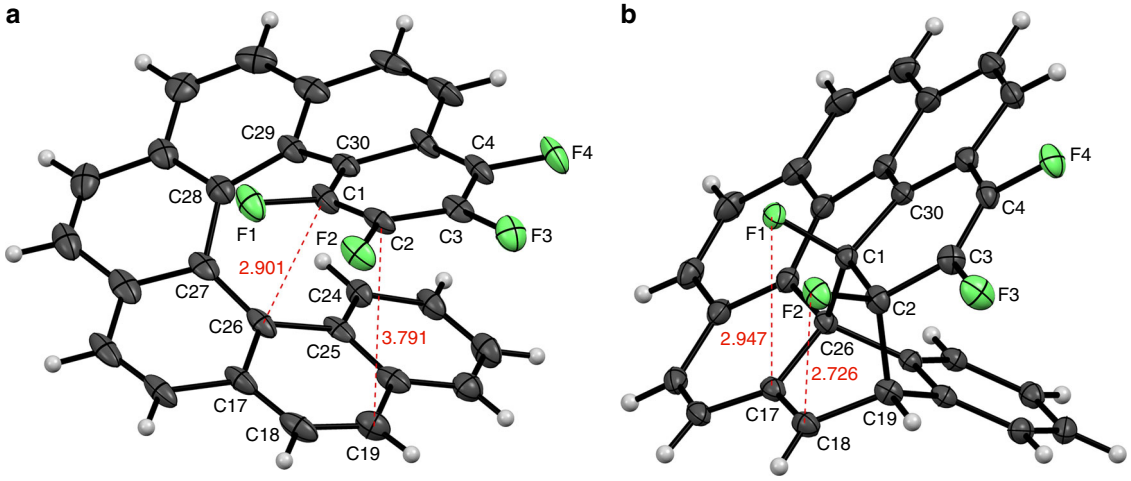

Fig. 3 Isolated intermediates **2** and **3** in the triple photochemical domino reaction. **a** ORTEP drawing of the X-ray crystal structure of **2** (thermal ellipsoids at the 50% probability level). Although four crystallographically independent molecules are present in the asymmetric unit (Supplementary Figure 1), only the molecule with the shortest C1···C26 contact (2.901 Å) is shown here. Selected interatomic distances (Å) and torsion angles (°): C1–F1, 1.349(5); C2–F2, 1.350(5); C3–F3, 1.337(6); C4–F4, 1.342(6); C1–C2, 1.348(8); C17–C18, 1.422(9); C18–C19, 1.344(7); C25–C26, 1.467(7); C17–C26, 1.416(7); C1–C26, 2.901 (6); C2–C19, 3.791(8); C24–C25–C26–C27, −17.2(8); C28–C29–C30–C1, −25.2(8). **b** ORTEP drawing of the X-ray crystal structure of **3** (thermal ellipsoids at the 50% probability level). Only one enantiomer is observed in the crystal structure owing to spontaneous resolution into the $P2_1$ non-centrosymmetric space group. Selected interatomic distances (Å) and torsion angles (°): C1–F1, 1.403(3); C2–F2, 1.401(2); C3–F3, 1.345(2); C4–F4, 1.355(2); C17–F1, 2.947 (2); C18–F2, 2.726(2); C1–C2, 1.572(3); C17–C18, 1.340(3); C18–C19, 1.511(2); C17–C26, 1.525(2); C1–C26, 1.552(2); C2–C19, 1.551(3); F1–C1–C2–F2, 9.5(2); F1–C1–C26–C17, −67.9(2); F2–C2–C19–C18, 56.5(2)

As a result of this cycloaddition, the bottom C17–C18 bond gains double bond character (1.340 Å). The vicinal F1 and F2 atoms of **3** are in close contact to the subjacent C=C bond (C17–F1, 2.947 Å; C18–F2, 2.726 Å, which are less than the sum of the van der Waals radii[25] of C and F, 3.17 Å) and ready to be transferred. As described above, X-ray visualisation of the domino process is thus possible for sequential photochemical reactions that go through thermally stable intermediates.

Photoirradiation of F_4-[7]helicene 2. With thermally stable intermediate **2** in hand, we next performed a double photochemical domino reaction and monitored the process by NMR spectroscopy (Supplementary Figures 6–8). The photochemical domino process at 50 °C in acetone-d_6 was faster than that in toluene-d_8, which suggests that the acetone solvent probably functions as a triplet sensitiser and promotes the substrate into the ππ* triplet state[26]. Although acetone is a better solvent for the double photochemical domino reaction starting from **2**, it is not suitable for the triple photochemical domino reaction starting from **1** owing to its reaction with **1** under photoirradiation to form an oxetane. Similar to photoinduced Diels–Alder reactions between anthracenes and dienophiles[27,28], the stepwise formation of two C–C bonds should occur in **2** as follows: the first C–C bond formation takes place in the inner helix between atoms with a shorter C···C distance (C1–C26, 2.901–2.935 Å; Fig. 3a and Supplementary Figure 1), then the second C–C bond formation closes the ring to afford **3**.

The observed photochemical Diels–Alder reactivity is specific to F_4-[7]helicene **2**. Neither F_4-[6]helicene[24] nor F_4-[8]helicene showed Diels–Alder reactivity under thermal or photochemical conditions (Supplementary Figures 10 and 11). It is known that intramolecular thermal Diels–Alder reactions of [7]helicene homologues require in situ generation of a benzyne intermediate[29], Lewis acid activation[19,30], or annealing at an extremely high temperature (~250 °C) on a metal surface[31].

Photoirradiation of Diels–Alder product 3. Using intermediate **3**, we verified the photoinduced double fluorine atom (2F) transfer from **3** to **4**. The *syn*-stereospecific 2F-transfer was swift and clean in acetone-d_6, and no further photochemical transformation occurred from **4** (Fig. 4). Because two C–F σ bonds and one C–C π bond participate in the 2F-transfer, it can be regarded as a formal $[2\sigma + 2\sigma + 2\pi]$-pericyclic reaction, known as a dyotropic rearrangement[32–36], which is an intramolecular process involving double group transfer reactions. Although the synthetic usefulness of 2H-dyotropic transfers is widely recognised and a photochemical 2H-dyotropic transfer[37] by triplet sensitisation is known, the corresponding 2F-dyotropic transfers have not yet been reported. Usually, thermal dyotropic rearrangements require

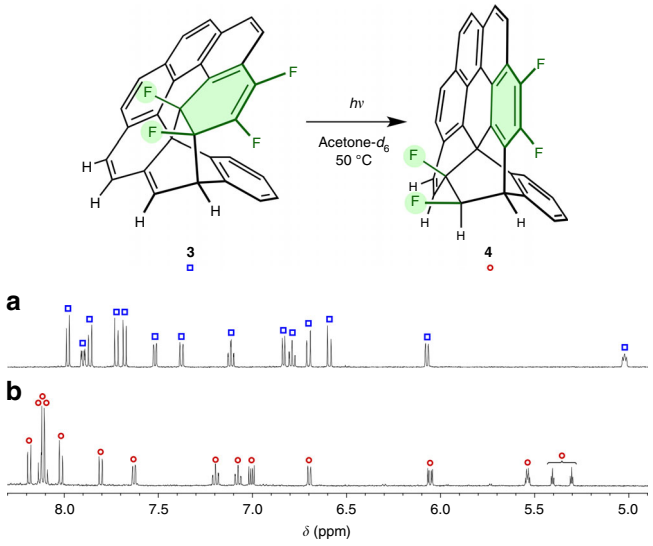

Fig. 4 Monitoring the photoinduced double fluorine atom transfer from **3** to **4**. An acetone-d_6 solution of **3** (2.2 mM) in an NMR tube was photoirradiated at 50 °C. ^{1}H NMR spectra (500 MHz, 298 K, acetone-d_6) of the sample solution are shown (**3**: blue squares, **4**: red circles). **a** Before irradiation. **b** After 5 min irradiation

high temperatures and proceed through a concerted pathway via a six-membered ring transition state with in-plane aromaticity[38,39]. However, considering that C–F bonds are markedly stronger than C–H bonds, overcoming the high energy penalty required to break two C–F bonds at the same time to form a six-membered ring transition state is unrealistic. In contrast, photochemical rearrangements proceed through a stepwise pathway with a biradical intermediate[37,40–42]. Aromatisation of the upper F_2-diene ring of **3** is the driving force for the stepwise 2F transfer; the first F transfer is somewhat advantageous for the outer F atom because of its shorter C···F migration distance (C18–F2, 2.726 Å; Fig. 3b).

Discussion

Using F_4-stilbene **1**, we performed a photoinduced domino reaction consisting of three photochemical steps: oxidative photocyclisation/photoinduced Diels–Alder reaction/photoinduced double group transfer reaction. Multiple photochemical domino reactions remain undeveloped[43–45] because domino reactions initiated by photoirradiation conventionally consist of consecutive thermal steps after the first photochemical step. One advantage of a photochemical domino process over a thermal one is that the domino process can be suspended and restarted at will simply by controlling the irradiation time. Therefore, we can confirm the domino process based on the X-ray crystal structures of isolated intermediates. The reaction sites generated at each domino step were highly organised and therefore smoothly brought about the subsequent intramolecular transformations under identical reaction conditions. Through the domino process from **1** to **4**, two vicinal fluorine atoms located on the terminal benzene ring of **1** were transferred onto the bicyclooctane framework of **4**.

Recently, the development of non-photochemical methods for the preparation of helicenes has attracted increasing attention[14,46]. However, if we had not applied the conventional oxidative photocyclisation method to prepare F_4-[7]helicene **2**, we would not have observed the unprecedented photoinduced 2F-transfer. It is worth further investigating this clean 2F-transfer in acetone from both practical and theoretical points of view.

Methods

General procedure for photochemical domino reaction. A toluene solution (500 mL) of F_4-stilbene **1** (45.4 mg, 0.0999 mmol, 0.20 mM), iodine (oxidant; 64.3 mg, 0.253 mmol, 2.5 equiv.) and propylene oxide (acid scavenger; 0.35 mL, 5.0 mmol, 50 equiv.) was bubbled with nitrogen gas for 15 min. A high-pressure Hg lamp (HB400X-15 400 W; SEN LIGHTS CORP) in a quartz water-cooling jacket was placed at the centre of a 500-mL reaction vessel containing the sample solution for internal irradiation. After sealing, the reaction vessel was immersed into an oil bath (PEG400) and the sample solution was heated at 50 °C with magnetic stirring. After UV light irradiation (the most prominent and efficient peak: 313 nm) at 50 °C for 10 min, the sample solution was cooled to room temperature and washed with an aqueous $Na_2S_2O_3$ solution to remove residual iodine. The organic layer was dried over anhydrous Na_2SO_4, filtered and concentrated in vacuo to afford a black oily residue. The crude product was directly purified by recycling preparative HPLC (GPC, eluent: $CHCl_3$) to afford pure product **4** (17.9 mg, 0.0397 mmol, 40%) as a light brown solid.

Intermediates **2** and **3** were obtained using the above procedure with a shorter irradiation time. After 2 min irradiation of **1** (46.1 mg, 0.101 mmol) in toluene (500 mL) at 50 °C, F_4-[7]helicene **2** was isolated as a light yellow solid (3.23 mg, 7.17×10^{-3} mmol) in 7% yield. Unreacted starting material **1** was recovered (34.6 mg, 0.0768 mmol, 75%) and used for another irradiation. After 5 min irradiation of **1** (45.6 mg, 0.100 mmol) in toluene (500 mL) at 50 °C, Diels–Alder product **3** was isolated as a yellow solid (6.33 mg, 1.41×10^{-2} mmol) in 14% yield. Unreacted **1**, F_4-[7]helicene **2** and 2F-transferred compound **4** were also obtained in 13, 18 and 8% yields, respectively.

Synthesis of 1–4, F_4-[6]helicene and F_4-[8]helicene. See Supplementary Methods.

X-ray crystallographic analyses. See Supplementary Methods and Supplementary Figures 1–3. The CIF and checkCIF files for compounds **2**–**4** are available as Supplementary Data 1-3 and 4-6 respectively.

Monitoring photochemical reactions. The ^{1}H NMR spectra for the triple photochemical domino reaction from **1** to **4** are shown in Supplementary Figures 4 and 5. The ^{1}H NMR spectra for the double photochemical domino reaction from **2** to **4** are shown in Supplementary Figures 6–8. The ^{1}H NMR spectra for the photoinduced double fluorine atom transfer from **3** to **4** are shown in Fig. 4 and Supplementary Figure 9. The ^{1}H NMR spectra of F_4-[6]helicene and F_4-[8]helicene after UV light irradiation are shown in Supplementary Figures 10 and 11, respectively.

Detailed NMR characterisation. See Supplementary Figures 12–19 for the precursor of **1**, Supplementary Figures 20–32 for (*E*,*Z*)-**1**, Supplementary Figures 33–36 for (*E*,*E*)-**1**, Supplementary Figures 37–50 for **2**, Supplementary Figures 51–65 for **3**, Supplementary Figures 66–81 for **4**, Supplementary Figures 82–98 for F_4-[6]helicene, and Supplementary Figures 99–111 for F_4-[8]helicene.

Data availability

The X-ray crystallographic coordinates for the structures of **2**–**4** are available as Supplementary Data 1–3, respectively. These data have also been deposited at the Cambridge Crystallographic Data Centre (CCDC), under deposition numbers CCDC 1865700 (**2**), 1865701 (**3**), and 1865703 (**4**). These data can be obtained free of charge from the CCDC via http://www.ccdc.cam.ac.uk/data_request/cif. All other data that support the findings of this study are available within the paper and its Supplementary Information, or are available from the corresponding author upon reasonable request.

Received: 28 October 2018 Accepted: 23 November 2018
Published online: 17 December 2018

References

1. Tietze, L. F. Domino reactions in organic synthesis. *Chem. Rev.* **96**, 115–136 (1996).
2. Tietze, L. F., Brasche, G. & Gericke, K. M. *Domino Reactions in Organic Synthesis* (Wiley-VCH, Weinheim, 2006).
3. Tietze, L. F. (ed) *Domino Reactions: Concepts for Efficient Organic Synthesis* (Wiley-VCH, Weinheim, 2014).
4. Wendt, K. U., Schulz, G. E., Corey, E. J. & Liu, D. R. Enzyme mechanisms for polycyclic triterpene formation. *Angew. Chem. Int. Ed.* **39**, 2812–2833 (2000).
5. Hoye, T. R., Baire, B., Niu, D., Willoughby, P. H. & Woods, B. P. The hexadehydro-Diels–Alder reaction. *Nature* **490**, 208–212 (2012).
6. Niu, D., Willoughby, P. H., Woods, B. P., Baire, B. & Hoye, T. R. Alkane desaturation by concerted double hydrogen atom transfer to benzyne. *Nature* **501**, 531–534 (2013).
7. Xu, F., Xiao, X. & Hoye, T. R. Photochemical hexadehydro-Diels–Alder reaction. *J. Am. Chem. Soc.* **139**, 8400–8403 (2017).
8. Xiao, X. & Hoye, T. R. The domino hexadehydro-Diels–Alder reaction transforms polyynes to benzynes to naphthynes to anthracynes to tetracynes (and beyond?). *Nat. Chem.* **10**, 838–844 (2018).
9. Kawamichi, T., Haneda, T., Kawano, M. & Fujita, M. X-ray observation of a transient hemiaminal trapped in a porous network. *Nature* **461**, 633–635 (2009).
10. Martin, R. H. The helicenes. *Angew. Chem. Int. Ed. Engl.* **13**, 649–660 (1974).
11. Shen, Y. & Chen, C.-F. Helicenes: synthesis and applications. *Chem. Rev.* **112**, 1463–1535 (2012).
12. Gingras, M. One hundred years of helicene chemistry. Part 1: non-stereoselective syntheses of carbohelicenes. *Chem. Soc. Rev.* **42**, 968–1006 (2013).
13. Hoffmann, N. Photochemical reactions applied to the synthesis of helicenes and helicene-like compounds. *J. Photochem. Photobiol. C* **19**, 1–19 (2014).
14. Chen, C.-F. & Shen, Y. (eds) *Helicene Chemistry: From Synthesis to Applications* (Springer-Verlag, Berlin/Heidelberg, 2017).
15. Mori, K., Murase, T. & Fujita, M. One-step synthesis of [16]helicene. *Angew. Chem. Int. Ed.* **54**, 6847–6851 (2015).
16. Beurskens, P. T., Beurskens, G. & van den Hark, T. E. M. Heptahelicene, $C_{30}H_{18}$. *Cryst. Struct. Commun.* **5**, 241–246 (1976).
17. van den Hark, T. E. M. & Beurskens, P. T. Heptahelicene, $C_{30}H_{18}$ (2nd modification). *Cryst. Struct. Commun.* **5**, 247–252 (1976).
18. Joly, M. et al. Bridged helicenes: 3,15-ethano- and 3,15-(2-oxapropano)-[7] helicene. Synthesis, proton NMR spectroscopy and X-ray diffraction study. *Helv. Chim. Acta* **60**, 537–560 (1977).
19. Fuchter, M. J., Weimar, M., Yang, X., Judge, D. K. & White, A. J. P. An unusual oxidative rearrangement of [7]-helicene. *Tetrahedron Lett.* **53**, 1108–1111 (2012).
20. Fujino, S. et al. Systematic investigations on fused π-system compounds of seven benzene rings prepared by photocyclization of diphenanthrylethenes. *Photochem. Photobiol. Sci.* **16**, 925–934 (2017).

21. Cho, D. M., Parkin, S. R. & Watson, M. D. Partial fluorination overcomes herringbone crystal packing in small polycyclic aromatics. *Org. Lett.* **7**, 1067–1068 (2005).
22. Cozzi, F., Bacchi, S., Filippini, G., Pilati, T. & Gavezzotti, A. Synthesis, X-ray diffraction and computational study of the crystal packing of polycyclic hydrocarbons featuring aromatic and perfluoroaromatic rings condensed in the same molecule: 1,2,3,4-tetrafluoronaphthalene, -anthracene and -phenanthrene. *Chem. Eur. J.* **13**, 7177–7184 (2007).
23. Kissel, P., Murray, D. J., Wulftange, W. J., Catalano, V. J. & King, B. T. A nanoporous two-dimensional polymer by single-crystal-to-single-crystal photopolymerization. *Nat. Chem.* **6**, 774–778 (2014).
24. Dračínský, M., Storch, J., Církva, V., Císařová, I. & Sýkora, J. Internal dynamics in helical molecules studied by X-ray diffraction, NMR spectroscopy and DFT calculations. *Phys. Chem. Chem. Phys.* **19**, 2900–2907 (2017).
25. Bondi, A. Van der Waals volumes and radii. *J. Phys. Chem.* **68**, 441–451 (1964).
26. Turro, N. J., Ramamurthy, V. & Scaiano, J. C. *Principles of Molecular Photochemistry: An Introduction* (University Science Books, Sausalito, 2009).
27. Sun, D., Hubig, S. M. & Kochi, J. K. Electron-transfer pathway for photoinduced Diels–Alder cycloadditions. *J. Photochem. Photobiol. A* **122**, 87–94 (1999).
28. Fukuzumi, S., Okamoto, T. & Ohkubo, K. Diels–Alder reactions of anthracenes with dienophiles via photoinduced electron transfer. *J. Phys. Chem. A* **107**, 5412–5418 (2003).
29. Zhigang, D., Katz, T. J., Golen, J. & Rheingold, A. L. Diels–Alder additions of benzynes within helicene skeletons. *J. Org. Chem.* **69**, 7769–7771 (2004).
30. Berger, R. J. F. et al. Gold(I) mediated rearrangement of [7]-helicene to give a benzo[*cd*]pyrenium cation embedded in a chiral framework. *Chem. Commun.* **50**, 5251–5253 (2014).
31. Stetsovych, O. et al. From helical to planar chirality by on-surface chemistry. *Nat. Chem.* **9**, 213–218 (2017).
32. Reetz, M. T. Dyotropic rearrangements, a new class of orbital-symmetry controlled reactions. Type I. *Angew. Chem. Int. Ed. Engl.* **11**, 129–130 (1972).
33. Reetz, M. T. Dyotropic rearrangements, a new class of orbital-symmetry controlled reactions. Type II. *Angew. Chem. Int. Ed. Engl.* **11**, 130–131 (1972).
34. Houk, K. N. et al. Mechanistic analysis of double hydrogen dyotropy in *syn*-sesquinorbornene disulfone. A combined kinetics and theoretical evaluation of primary deuterium isotope effects. *J. Am. Chem. Soc.* **116**, 10895–10913 (1994).
35. Fernández, I., Cossío, F. & Sierra, M. A. Dyotropic reactions: mechanisms and synthetic applications. *Chem. Rev.* **109**, 6687–6711 (2009).
36. Fernández, I. & Bickelhaupt, F. M. The activation strain model and molecular orbital theory: understanding and designing chemical reactions. *Chem. Soc. Rev.* **43**, 4953–4967 (2014).
37. Wölfle, I., Chan, S. & Schuster, G. B. The triplex Diels–Alder reaction: intramolecular cycloaddition of phenyl-substituted alkenes to 1,3-dienes. *J. Org. Chem.* **56**, 7313–7319 (1991).
38. Fernández, I., Sierra, M. A. & Cossío, F. P. In-plane aromaticity in double group transfer reactions. *J. Org. Chem.* **72**, 1488–1491 (2007).
39. Fernández, I., Bickelhaupt, F. M. & Cossío, F. P. Double group transfer reactions: role of activation strain and aromaticity in reaction barriers. *Chem. Eur. J.* **15**, 13022–13032 (2009).
40. Sierra, M. et al. Light-induced aminocarbene to imine dyotropic rearrangement in a chromium(0) center: an unprecedented reaction pathway. *J. Am. Chem. Soc.* **125**, 9572–9573 (2003).
41. Fernández, I., Sierra, M. A., Gómez-Gallego, M., Mancheño, M. J. & Cossío, F. P. The photochemical reactivity of the "photo-inert" tungsten (Fischer) carbene complexes. *Angew. Chem. Int. Ed.* **45**, 125–128 (2006).
42. Fernández, I., Sierra, M. A., Mancheño, M. J., Gómez-Gallego, M. & Cossío, F. P. The noncarbonylative photochemistry of group 6 Fischer carbene complexes. *Eur. J. Inorg. Chem.* 2454–2462 (2008).
43. Kitamura, T., Kobayashi, S. & Taniguchi, H. Photochemistry of vinyl halides. Heterocycles from reaction of photogenerated vinyl cations with azide anion. *J. Org. Chem.* **49**, 4755–4760 (1984).
44. Basarić, N. et al. Novel 2,4-methanoadamantane-benzazepine by domino photochemistry of *N*-(1-adamantyl)phthalimide. *Org. Lett.* **10**, 3965–3968 (2008).
45. Horvat, M. et al. Photoinitiated domino reactions: *N*-(adamantyl)phthalimides and *N*-(adamantylalkyl)phthalimides. *J. Org. Chem.* **74**, 8219–8231 (2009).
46. Nejedlý, J. et al. Synthesis of long oxahelicenes by polycyclization in a flowreactor. *Angew. Chem. Int. Ed.* **56**, 5839–5843 (2017).

Acknowledgements

This work was supported by The Foundation for Japanese Chemical Research (No. 461 (R)) and performed under the Cooperative Research Program of the "Network Joint Research Center for Materials and Devices" (No. 20171175 and 20181185).

Author contributions

T. M. conceived the concept and directed the project. T. M. and C. M. designed and carried out the experiments. K. A. and T. S. conducted the X-ray crystal structure analyses. T. M. and C. M. wrote the manuscript with input from K. A., T. S., and M. F.

Additional information

Supplementary information accompanies this paper at https://doi.org/10.1038/s42004-018-0099-7.

Competing interests: The authors declare no competing interests.

Reprints and permission information is available online at http://npg.nature.com/reprintsandpermissions/

Publisher's note: Springer Nature remains neutral with regard to jurisdictional claims in published maps and institutional affiliations.